The Company of **Biologists**

RESEARCH ARTICLE

Spindly is required for rapid migration of human cells

Claudia Conte[1],[*],[§], Michelle A. Baird[2], Michael W. Davidson[2] and Eric R. Griffis[1],[‡],[§]

ABSTRACT

Dynein is the sole processive minus-end-directed microtubule motor found in animals. It has roles in cell division, membrane trafficking, and cell migration. Together with dynactin, dynein regulates centrosomal orientation to establish and maintain cell polarity, controls focal adhesion turnover and anchors microtubules at the leading edge. In higher eukaryotes, dynein/dynactin requires additional components such as Bicaudal D to form an active motor complex and for regulating its cellular localization. Spindly is a protein that targets dynein/dynactin to kinetochores in mitosis and can activate its motility *in vitro*. However, no role for Spindly in interphase dynein/dynactin function has been found. We show that Spindly binds to the cell cortex and microtubule tips and colocalizes with dynein/dynactin at the leading edge of migrating U2OS cells and primary fibroblasts. U2OS cells that lack Spindly migrated slower in 2D than control cells, although centrosome polarization appeared to happen properly in the absence of Spindly. Re-expression of Spindly rescues migration, but the expression of a mutant, which is defective for dynactin binding, failed to rescue this defect. Taken together, these data demonstrate that Spindly plays an important role in mediating a subset of dynein/dynactin's function in cell migration.

KEY WORDS: Dynein/Dynactin, Kinetochore, Migration

INTRODUCTION

Cell migration is required for development and homeostasis in almost all multi-cellular organisms. The activation of this process requires specific stimuli from growth factors, chemokines or extracellular matrix molecules, which activate specific receptors and signalling cascades (Ridley, 2011). To migrate in 2-dimensions, a cell must protrude its plasma membrane, anchor these protrusions to the underlying substrate, and then use these connections to pull the cell body forward while constricting the rear of the cell and disassembling and releasing old connections (Krause and Gautreau, 2014). This process therefore requires the careful coordination between adhesive complexes, cytoskeletal filament systems with their attendant motor proteins, the secretory/membrane transport machinery and the regulatory molecules that control the activities of

these disparate networks (Schmoranzer et al., 2003; Kaverina and Straube, 2011; Huber et al., 2015).

Actin microfilaments and non-muscle myosin II provide the majority of forces that drive migration. At the leading edge, small GTPases control the nucleation of actin filaments through the Arp2/3 complex, which produces branched filaments, and formin/Spire/JMY proteins, which build unbranched filaments (Ridley, 2011; Campellone and Welch, 2010; Firat-Karalar and Welch, 2011). The polymerization of actin at the leading edge of migrating cells generates the force to drive the extension of the cell membrane. Within the cell, bundled actin filaments, attached to focal adhesions, provide cables for the generation of traction forces that propel the cell body forward; at the rear of the cell, myosin contraction of actin filaments leads to the retraction of the cell body and release of focal adhesions (Ridley, 2011; Parsons et al., 2010; Aratyn-Schaus et al., 2011).

Although they do not themselves generate forces, microtubules are essential in many cell types for polarization and for regulating the speed of migration, and there are many points of feedback where microtubules, focal adhesions, and the actin network influence each other (Vasiliev et al., 1970; Kaverina and Straube, 2011; Stehbens and Wittmann, 2012; Akhshi et al., 2014). After an initial migration cue is received in a fibroblast, the microtubule organizing centre (MTOC) orients itself between the nucleus and a cell's leading edge and projects dynamic microtubules towards the lamellipodium (Magdalena et al., 2003; Gomes et al., 2005; Gotlieb et al., 1981, 1983). These microtubules provide the tracks upon which membrane vesicles and locally translated mRNAs travel and deliver GTPase regulating proteins that activate Rac and Rho to stimulate focal adhesion internalization, actin polymerization or cell contraction (Rogers et al., 2004; Krendel et al., 2002; Rooney et al., 2010; Waterman-Storer et al., 1999; Montenegro-Venegas et al., 2010; Yadav et al., 2009; Mingle et al., 2005). There are also direct interactions between the actin cytoskeleton and microtubules through proteins such as the spectraplakin ACF7/MACF1 that can link microtubules to focal adhesions, the formin mDia1 that nucleates actin filaments and also stabilizes microtubules, and IQGAP1, which binds to several microtubule plus-tip proteins and can regulate actin and myosin activities (Palazzo et al., 2001a; Bernier et al., 2000; Karakesisoglou et al., 2000; Brandt and Grosse, 2007). Finally, motors of the kinesin superfamily are able to regulate microtubule dynamics, network architecture, and cargo transport and therefore many of them have roles in cell migration [for review see (Bachmann and Straube, 2015)].

As the only processive minus-end-directed microtubule motor, the dynein/dynactin supercomplex also has well established roles in cell migration. Dynein is targeted to growing microtubule plus-ends via the p150 subunit of dynactin, which is itself recruited by proteins, such as EB1 and CLIP-170, that bind to the plus-ends of microtubules and regulate their dynamics (Folker et al., 2005; Duellberg et al., 2014; Valetti et al., 1999; Vaughan et al., 1999, 2002). The dynein/dynactin complex was also described to be involved in cytoskeleton reorganisation upon wounding and in

[1]Centre for Gene Regulation and Expression, College of Life Sciences, University of Dundee, Dundee DD1 5EH, UK. [2]Department of Biological Science, National High Magnetic Field Laboratory, Florida State University, Tallahassee, FL 32306, USA. *Present address: Department of Cell and Developmental Biology, Centre for Genomic Regulation (CRG), The Barcelona Institute of Science and Technology, 08003 Barcelona, Spain. ‡Present address: Nikon Instruments Inc, 1300 Walt Whitman Road, Melville, NY 11747, USA.

§Authors for correspondence (eric.griffis@nikon.com; claudia.conte@crg.eu)

C.C., 0000-0002-3547-8085; E.R.G., 0000-0002-2832-6649

directed cell movement (Palazzo et al., 2001b; Faulkner et al., 2000; Smith et al., 2000). In addition to the dynein and dynactin complexes, several accessory factors, such as Lis1 and Ndel1, are important for the activity of the motor in many contexts, including cell migration (Cianfrocco et al., 2015; Reiner et al., 1993). Recent research has shown that vertebrate dynein and dynactin do not form a processive motor complex without activating factors such as Bicaudal-D (BicD) or Hook3. These activating factors drive dynein/dynactin supercomplex formation and allow it to move on microtubules (McKenney et al., 2014; Schlager et al., 2014; Urnavicius et al., 2015). Spindly has been shown to be one such activating factor (McKenney et al., 2014).

Spindly was identified through two RNAi screens in *Drosophila melanogaster* S2 cells in which mitotic and interphase phenotypes were analysed. In interphase cells, Spindly depletion generated alterations in cytoskeletal architecture with spiky and elongated microtubule-rich projections in contrast to the normal smooth, rounded S2 cells. Moreover, GFP-Spindly was shown to track on the plus-ends of interphase microtubules, where it colocalized with the canonical plus-end binding protein EB1 (Griffis et al., 2007).

After the initial study in 2007, all of the subsequent publications on Spindly have been focused on describing its role during mitosis in human cells and worms (Gassmann et al., 2008, 2010; Holland et al., 2015; Yamamoto et al., 2008; Barisic et al., 2010; Cheerambathur et al., 2013; Chan et al., 2009; Moudgil et al., 2015); thus it was unclear whether Spindly in other organisms plays any functions in interphase cells.

In this study, we identified a direct role of human Spindly in wound healing and cell movement. Although predominantly a nuclear protein, Spindly localizes at the leading edge and focal adhesions in migratory cells. Cells lacking Spindly are slow to migrate in a scratch-wound assay, a defect that can be rescued by the reintroduction of the wild-type protein but not by the expression of a mutant that fails to bind to dynactin. Therefore, we can conclude that Spindly's role in cell migration is likely due to its function in regulating dynein/dynactin activity, similar to its established role in mitosis. These results delineate for the first time an interphase role for Spindly and confirm that this protein is a key adaptor for the dynein/dynactin motor complex in multiple cellular processes and in different cell cycle phases.

RESULTS AND DISCUSSION
Localisation of human Spindly in fixed non-mitotic cells

To date, there has been very little data on human Spindly in non-mitotic cells, and so we began by assessing its localization. When we used an affinity-purified antibody raised against the full-length recombinant protein to stain U2OS cells that were grown in a monolayer and then scratched to induce cell migration, we noticed that, in addition to the expected nuclear staining, there was also a cytoplasmic pool of protein (Fig. 1A, upper). We confirmed the specificity of this staining by observing that siRNA depletion of Spindly eliminated the staining (Fig. 1A, lower and B). Fractionation of cells into nuclear and cytoplasmic fractions followed by western blotting demonstrated the presence of Spindly in both compartments (Fig. 1C; Fig. S1).

To examine Spindly's localization in a more migratory cell type and to determine if it localizes with any components of the dynein/dynactin complex, we fixed and stained primary human fibroblasts
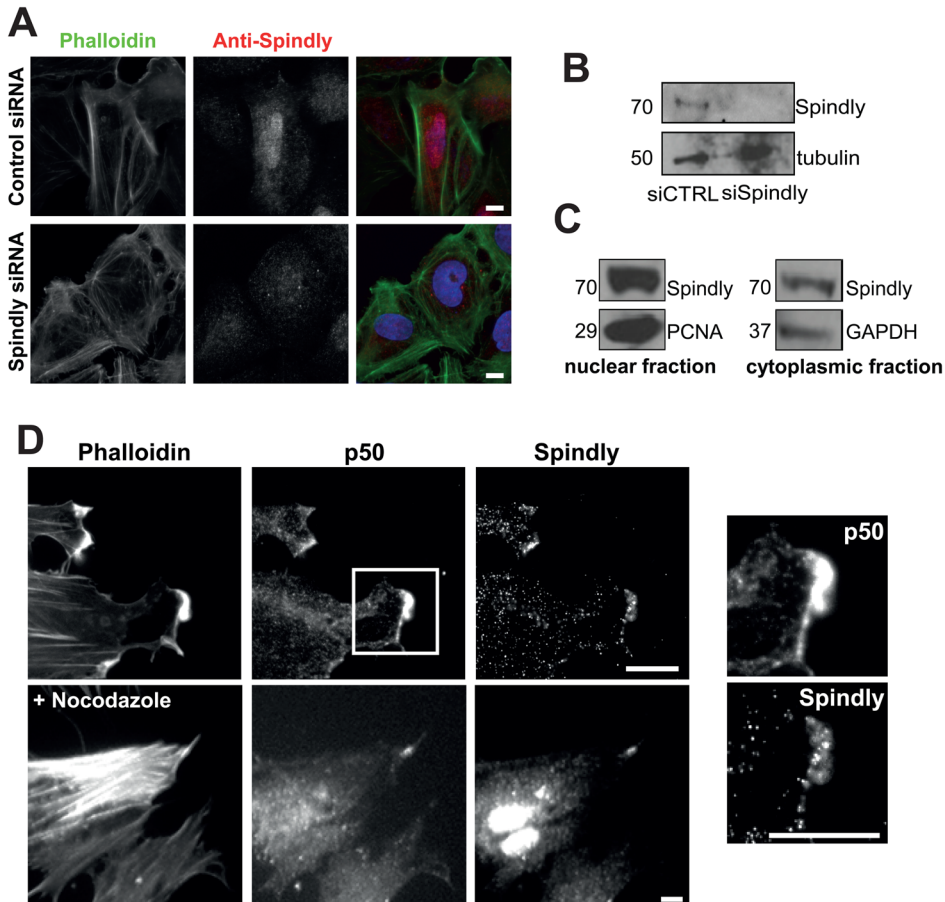

Fig. 1. Spindly localizes to the leading edge of fixed migrating cells.
(A) Confluent U2OS cells were treated with control or Spindly-specific siRNAs and then cells were fixed and stained to visualize nuclei (DAPI), filamentous actin (phalloidin) and Spindly. (B) An immunoblot of cell lysates show that Spindly was efficiently depleted by the siRNAs. (C) U2OS cells were lysed and the cytoplasmic and nuclear fractions were separated. Co-fractionation with PCNA confirms Spindly presence in the nucleus and co-fractionation with GAPDH confirms the presence of Spindly in the cytoplasm. (D) Foreskin fibroblasts were cultured to confluency, and then the monolayer was scratched to promote cell migration. 4 h after scratch-wounding, cells were fixed and stained to visualize filamentous actin (phalloidin), p50 Dynamitin, and Spindly. Images on the left show a magnification of the box shown in the upper image. Nocodazole treatment did not abolish the colocalization of p50 and Spindly. Scale bars: 10 µm.

to visualize filamentous actin, the p50-Dynamitin subunit of dynactin and Spindly (Fig. 1D). We clearly observed that Spindly and p50 colocalized at the leading edge of these cells (Fig. 1D, lower panels). This colocalization was abolished by the application of latrunculin B (Fig. S2), but remained in cells treated with nocodazole to depolymerize microtubules (Fig. 1E), suggesting that the proteins were associating with an actin-based structure.

Live-cell imaging reveals that Spindly localizes to microtubule tips and mature focal adhesions

To further explore Spindly's localization in interphase we asked whether Spindly could be seen associating with the basal cell cortex and/or cytoskeletal elements. We therefore imaged U2OS cells stably and inducibly expressing low levels of GFP-Spindly using total internal reflection fluorescence (TIRF) microscopy. TIRF allowed us to strictly visualize the localization of Spindly on or near the cell cortex, without interference from the nuclear signal, which is dominant in wide-field microscopy. In TIRF, we observed that there was a consistently bright fluorescent signal at the basal cortex. Additionally, we observed multiple populations of GFP-Spindly foci on the cortex. Some appeared to be moving diffusively, while others were more stable over multiple frames and appeared to be on cytoskeletal structures and in cytoplasmic projections (Fig. 2A and Movie 1). In order to better understand how Spindly localizes in

migrating cells, we visualized Spindly in U2OS cells that were grown to confluency and then scratch-wounded to induce cell migration. We observed that Spindly associated with the basal surface of the expanding plasma membrane and in rapidly moving foci (Movie 2).

To determine if the foci of Spindly were associated with microtubule plus-ends, we transfected our GFP-Spindly expressing U2OS cell line with TagBFP2-Tubulin and imaged these cells with TIRF. A small fraction of the observed particles of GFP-Spindly were clearly associated with microtubule plus-ends. The example shown in Fig. 2B and Movie 3 contains a Spindly focus that remains on a microtubule that retracts and then grows over 10 s.

To further analyse the leading edge localisation of Spindly and its dynamics, we co-transfected our U2OS cells with RFP-Zyxin to visualize focal adhesions. Upon scratch-wounding, we followed the cells using TIRF microscopy. Fig. 2C shows the recruitment of Spindly to the leading edge in these moving cells. We observed that it enriched with Zyxin, but only significantly after migration and Zyxin redistribution had begun (Movie 4). This indicates that Spindly could potentially require focal adhesion maturation to be recruited or be involved in the later stages of focal adhesion maturation or turnover (Nagano et al., 2012). Furthermore, in fixed cells we also observed the colocalization of endogenous Spindly and RFP-Zyxin at focal adhesions at the cell periphery (Fig. S3).
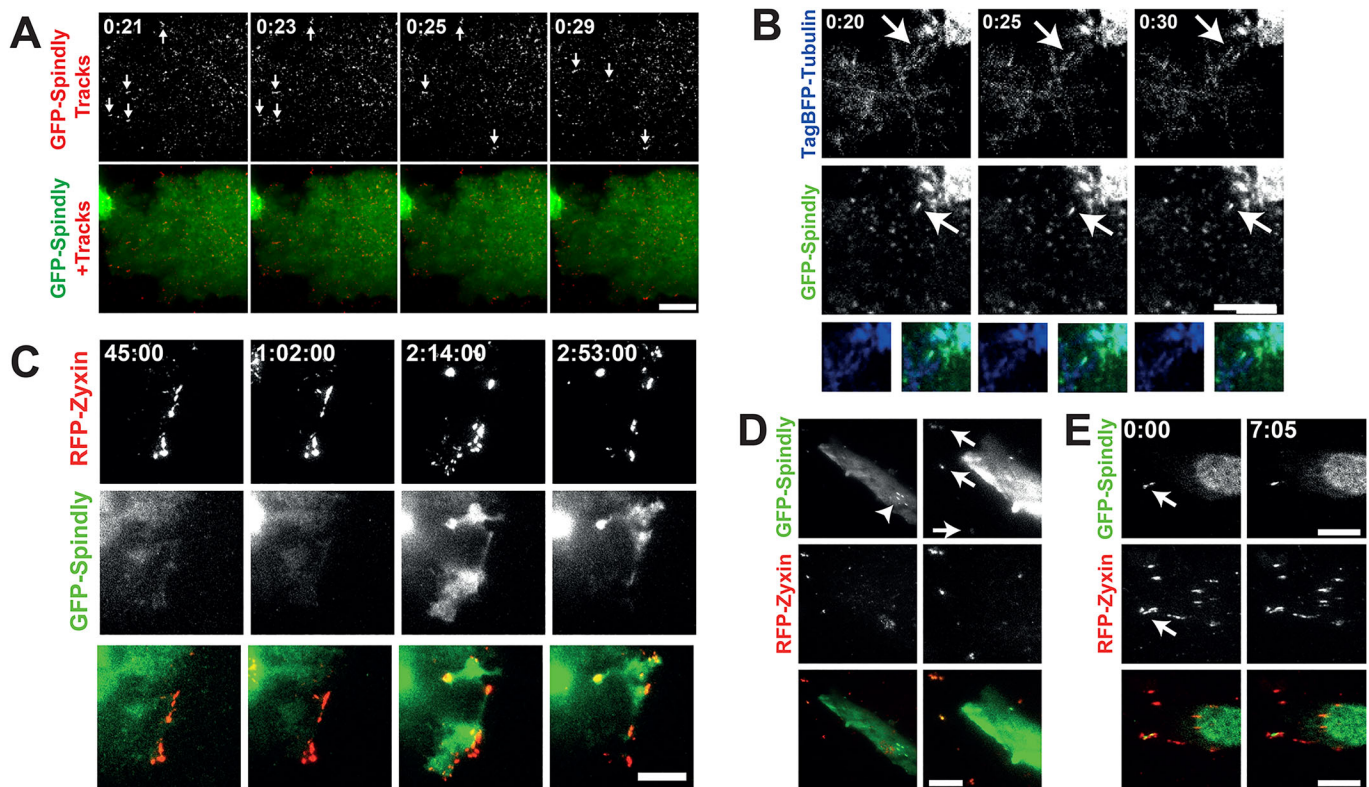

Fig. 2. Spindly can be seen moving on the basal cell cortex and associated with microtubule plus-ends. (A) U2OS cells stably expressing low levels of GFP-Spindly were imaged with total internal reflection fluorescence microscopy (TIRF). To better visualize the movement of individual particles across multiple images, a Gaussian filter was applied to de-noise the images, and then a temporal filter was used to find foci that were moving across multiple images that were compiled into trails. Arrows show moving GFP-Spindly. The lower image shows the particle trails (red) overlaid on top of the still GFP-Spindly image. Time is minutes:seconds. (B) The same U2OS cells as in A were transfected with TagBFP2-Tubulin and imaged in TIRF. The arrow shows a TagBFP2-labeled microtubule that shrinks and grows over the course of imaging. Time is minutes:seconds. (C) The same U2OS cells were transfected with RFP-Zyxin, grown to confluency and then induced to migrate. GFP-Spindly only began to co-localize at the leading edge at 45 min post scratch-wounding. Time is shown in hours:minutes:seconds. (D) Fibroblasts were transiently transfected with GFP-Spindly and RFP-Zyxin and then imaged in TIRF. Arrows show focal adhesions where Spindly and Zyxin colocalize, which are more obvious in the first frame where the brightness was enhanced relative to the other time points. The arrowhead shows filaments of GFP-Spindly. (E) In another fibroblast, a focus of GFP-Spindly was observed (arrow) that was dynamically associated with focal adhesions. Time is shown in minutes:seconds. Scale bars: 10 μm.

When we co-transfected GFP-Spindly and RFP-Zyxin into resting fibroblasts, we also observed that some GFP-Spindly colocalized with RFP-Zyxin at focal adhesions (Fig. 2D). However, the loss of Spindly did not seem to affect the size, number, or distribution of focal adhesions in U2OS cells (data not shown).

Seeing human Spindly on microtubule tips and identifying new pools of Spindly in interphase cells raised the possibility of a novel cytoskeletal role for this protein, a function different from the already established mitotic role.

Spindly is required for cell migration

Given that we observed Spindly on microtubule tips and focal adhesions in the cytoplasm of interphase cells, and that we know that it can interact with the dynein/dynactin complex that is essential for promoting rapid cell migration, we sought to determine whether Spindly might also be involved in the cell migration process. We therefore carried out a scratch assay to study two-dimensional cell migration in Spindly-depleted cells. This method is based on the generation of an artificial gap or wound in a monolayer of cells that will drive the movement of cells on the edge of the wound to close the gap.

We silenced Spindly expression in U2OS cells by treatment with specific siRNAs for 96 h and then seeded cells into two small wells separated by a silicon wall. Once confluence was reached, the insert was removed, generating a reproducible gap in the monolayer of cells (Fig. 3A). We followed the movement of the cells on the wound edge by live imaging for at least 24 h and then analysed the movies by measuring the width of the wound over time (Fig. 3B). In multiple independent experiments, cells depleted of Spindly (typical results shown in Fig. 3C) showed slow closure rates and typically were not able to close the gap after 24 h (Fig. 3B). Previous work has shown that Spindly interacts with the dynein/dynactin complex (McKenney et al., 2014), and interestingly, depletion of two separate subunits of Dynactin, p150 and p50, retards wound closure migration rates (Fig. S4) comparable to Spindly-depleted cells.

Because Spindly-depleted cells are defective in division and do not proliferate as well as control cells, we wished to exclude the possibility that the migration phenotype that we observed was caused by defects in cell proliferation. We therefore synchronised cells in S phase by administering Hydroxyurea (HU; 1 mM) for 24 h and repeated the scratch assay. The stabilization of geminin (Fig. 3D) confirmed that the HU treatment was blocking cell cycle progression (McGarry and Kirschner, 1998). When we observed the control HU-treated and the Spindly-depleted HU-treated cells, we found that the Spindly-depleted cells HU treated were still slower to close the scratch wound.
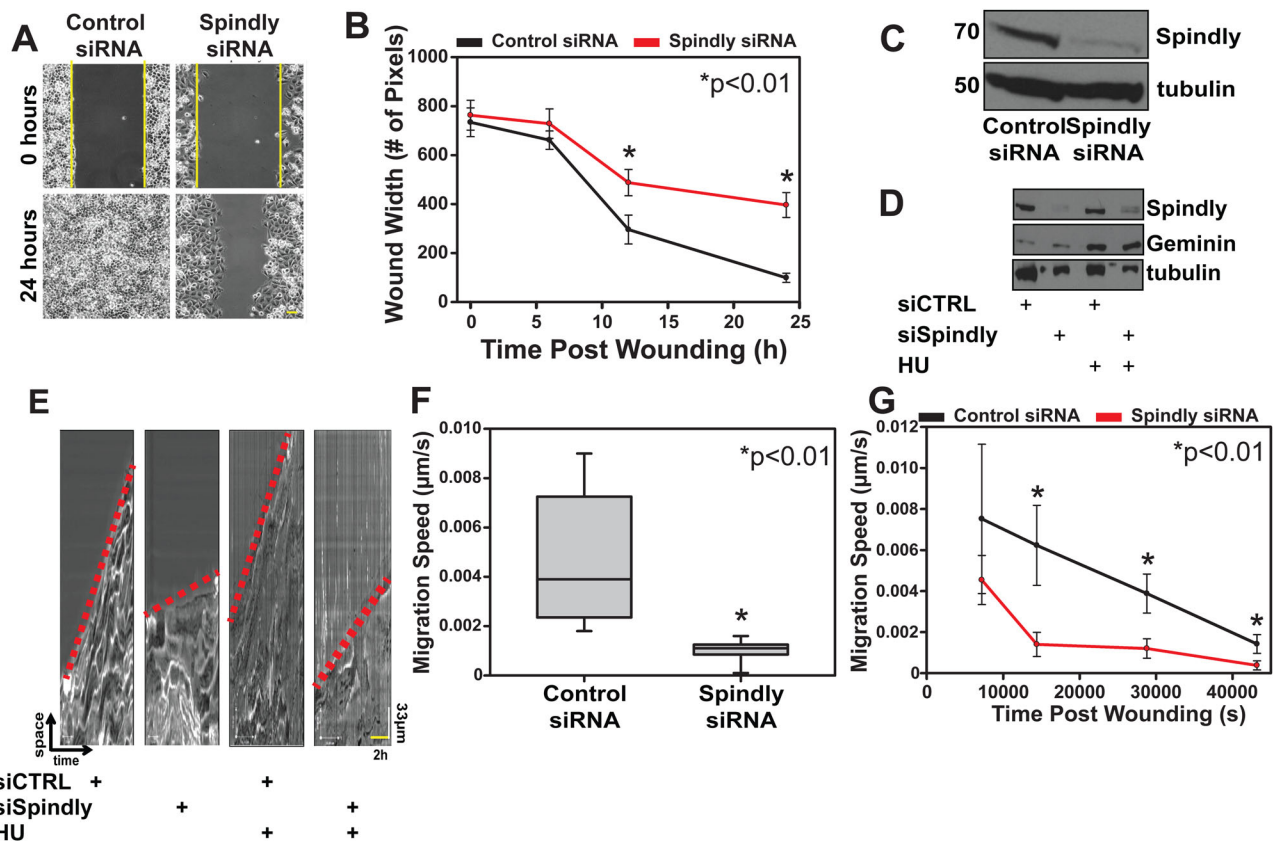

Fig. 3. Spindly is required for rapid cell migration. (A,B) U2OS cells treated with control or Spindly-specific siRNAs were plated into an ibidi silicone culture-insert inside an imaging chamber. After cells reached confluency, the insert was removed and the closure of the induced wound was followed over time using phase-contrast microscopy. Three independent experiments were performed and data in the graph represent mean±s.d. (C) Western blotting confirmed that the Spindly-specific siRNAs were effective at depleting the protein. (D) Spindly siRNA and control siRNA treated cells were treated with hydroxyurea (HU) to block DNA synthesis and arrest cells at the entry of S-phase. Geminin protein levels confirmed that the HU treatment worked. Tubulin used as loading control. (E–G) Kymographs generated from control and Spindly-depleted cells migration movies. Red dotted lines to indicate the different slopes (i.e. velocity) between control and silenced cells. The kymographs were used to measure the speed of cells at various time points post wounding. The Spindly-silenced cells were slower to migrate into a wound, regardless of whether or not HU was added to the cells. Three independent experiments were performed and data in the graph represent mean±s.d. Student's t-test was used to determine the statistical significance.

We used kymographs to analyse the speed of cells migrating into the wound (Fig. 3E) and found that the Spindly-depleted cells were slower than the control cells, regardless of whether or not cells had been treated with HU prior to wounding (Fig. 3F). When we measured the velocity starting at different temporal points after wounding, we confirmed that the Spindly-depleted cells were moving slower than the controls at each time point.

To demonstrate that this phenotype was strictly due to a lack of Spindly expression, we generated a stable cell line expressing a siRNA-resistant, tet-inducible GFP-Spindly to allow the re-expression of Spindly after siRNA depletion of the endogenous protein. Fig. 4A–C shows that re-expressing an exogenous copy of Spindly rescued the migration phenotype; cells expressing wild-type GFP-Spindly showed a rate of wound closure similar to control cells, even though the overall amount of GFP-Spindly was lower than the combined level of endogenous and GFP-Spindly expressed in control siRNA treated cells. This experiment provides further evidence that Spindly-depleted cells are intrinsically defective in cell migration, and that the defects we measure are not produced by off-target effects of the siRNAs used.

We next wanted to determine if the non-mitotic Spindly function could be due to its association with the dynein/dynactin motor complex. To test this, we generated a stable cell line expressing a siRNA-resistant GFP-Spindly where serine 256 is mutated to alanine, a mutation that abolishes the ability of the protein to bind to dynactin (as previously described, Gassmann et al., 2010). We depleted the endogenous form of the protein and repeated the rescue

experiment with cells that now inducibly express GFP-Spindly S256A. The expression of this mutant in the absence of the endogenous protein did not rescue the wound closure rate to control levels (Fig. 4D–F). From this data we hypothesize that Spindly is playing a role in cell migration via regulation of the dynein/dynactin motor complex.

Spindly depletion does not grossly affect the distribution of myosin or actin filaments or centrosomal re-orientation in migrating cells

There was the possibility that the depletion of Spindly from migrating U2OS cells could dramatically alter the actin-myosin or microtubule cytoskeleton as it did in *Drosophila* S2 cells, leading to the slow migration phenotype (Griffis et al., 2007). To check this, we fixed and stained migrating control siRNA-treated and Spindly-depleted cells with fluorescent phalloidin and an antibody that recognizes the phosphorylated (active) form of the myosin regulatory light chain. We did not observe any gross defects in the organization of actin filaments and active myosin in these cells, although there was a trend towards lower levels of phospho-myosin in Spindly-depleted cells (Fig. 5A).

An important step in polarizing migrating cells is the re-orientation of centrosomes towards the leading edge, which is a dynein/dynactin dependent process and occurs after wounding (Schmoranzer et al., 2009). We wished to determine if this process was compromised in cells lacking Spindly, and so we fixed and stained control and Spindly-depleted cells 4 h after scratch-wounding to visualize
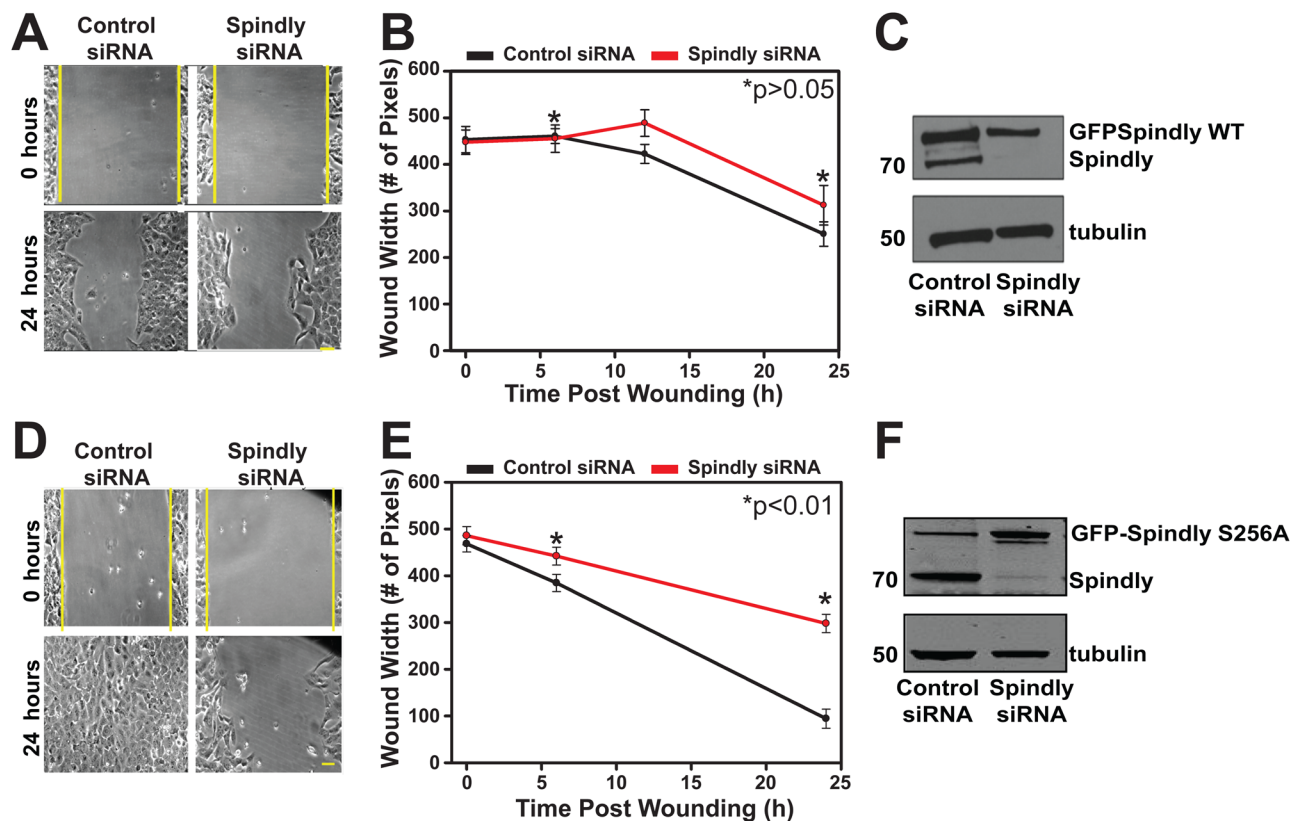

Fig. 4. Spindly requires an interaction with dynactin to promote cell migration. U2OS cells stably expressing either wild-type (WT) (A–C) or mutant S256A (D–F) GFP-Spindly under the control of doxycycline were treated with control siRNAs or siRNAs that targets the endogenous Spindly. (A–C) The expression of close to endogenous levels of GFP-Spindly WT was sufficient to nearly completely rescue wound closure. (D–F) The expression of a GFP-Spindly mutant (S256A), which impairs its interaction with dynactin, was not sufficient to rescue the migration velocity rate. Student's *t*-test was used to determine the statistical significance.
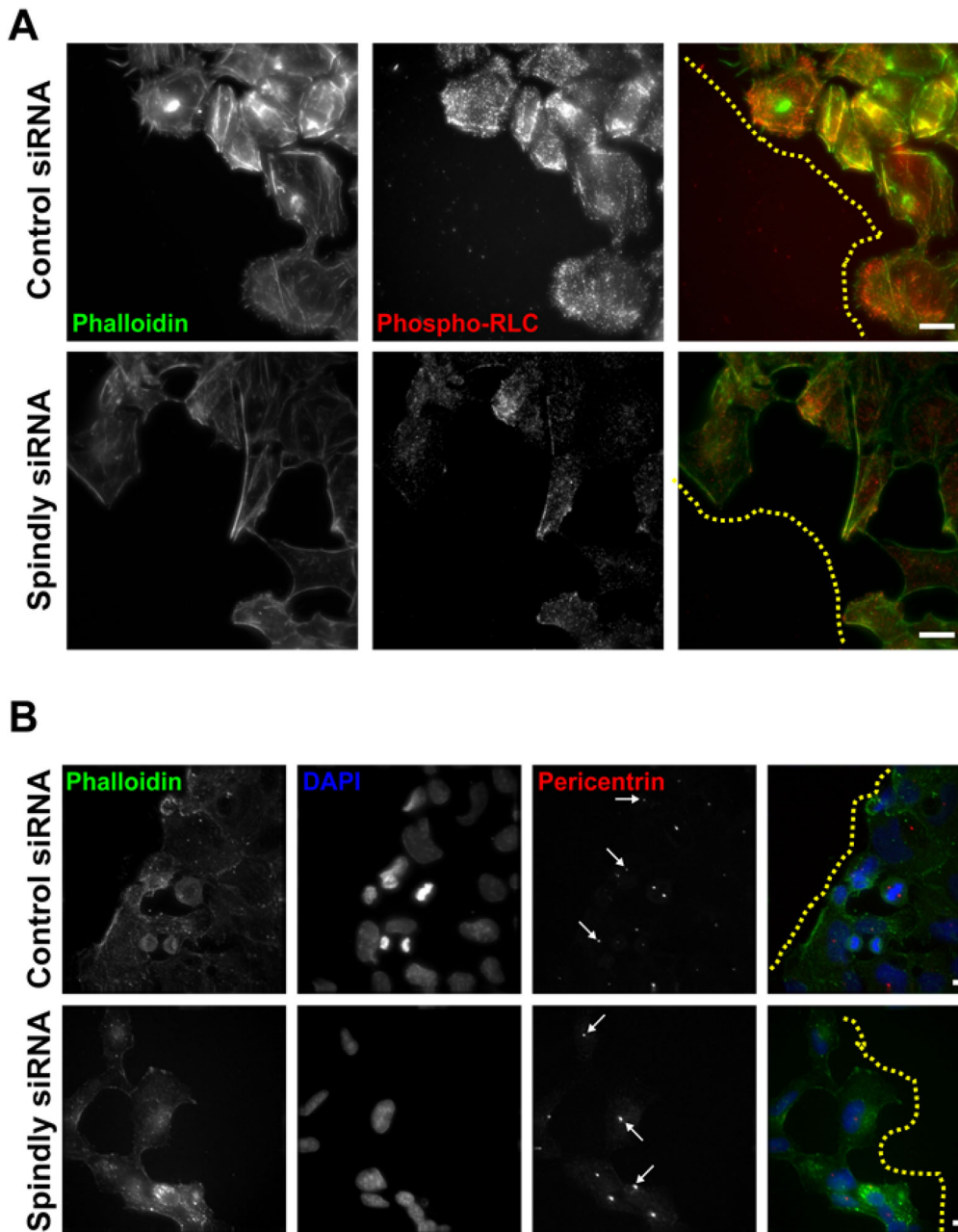
Fig. 5. Cells lacking Spindly do not show dramatic alterations in their actomyosin cytoskeleton or in their ability to re-orient their centrosomes as they migrate. (A) Confluent U2OS cells that had been treated with the given siRNAs were wounded and then fixed and stained to visualize actin filaments and the active form of the RLC. Yellow dotted lines are to limit the leading edge of the cell sheet. (B) Cells treated in a similar manner as in A were fixed and stained to visualize filamentous actin, nuclei, and centrosomes. Arrows show cells where the centrosome has been reoriented and is lying between the nucleus and the leading edge. Scale bars: 20 µm.

centrosomes and nuclei. We saw many examples of Spindly-depleted cells at the wound edge where the centrosomes were oriented correctly between leading edges and nuclei (Fig. 5B). We therefore conclude that the migration defects that we observed in the Spindly-depleted cells are dynein/dynactin dependent, but they are not caused by a wholesale loss of dynein/dynactin function. This is in keeping with previous results, where we found that the depletion of Spindly did not cause the redistribution of Rab5-positive early endosomes in interphase S2 cells that was seen when dynein was depleted (Griffis et al., 2007).

Spindly first emerged as a protein in human, *Drosophila* and *C. elegans* that is required for the recruitment of dynein/dynactin to kinetochores (Griffis et al., 2007; Gassmann et al., 2008; Yamamoto et al., 2008). However, other functions for Spindly appeared to have diverged. In human cells and *C. elegans*, the depletion of Spindly led to severe chromosome alignment phenotypes, but did not inhibit the shedding of spindle assembly

checkpoint (SAC) proteins from aligned kinetochores (Griffis et al., 2007; Gassmann et al., 2008). In contrast, the depletion of Spindly from *Drosophila* cells did not markedly inhibit chromosome alignment, but did lead to the accumulation of SAC proteins on aligned kinetochores (Griffis et al., 2007). How much of these differences are due to species-specific changes in the mechanisms of SAC silencing or the roles of dynein/dynactin has yet to be determined. Recent work showed that dynein/dynactin complex formation and processivity is facilitated by accessory factors like Spindly, which control the localization, activation and/or cargo-binding of the complex (Schroeder and Vale, 2016; Schlager et al., 2014; McKenney et al., 2014).

Just as the role of Spindly in mitotic cells appeared to be different among different species there is also an interesting bifurcation in Spindly's interphase function. In human cells, the protein appeared to be almost exclusively nuclear, while in *Drosophila* cells, Spindly bound to microtubule plus-ends and its depletion produced a

striking morphological phenotype (Griffis et al., 2007). *Drosophila* Spindly is 175 amino acids longer than the human protein and contains four clusters of positively charged residues (consensus sequence: TPAKPQ-L/R/M-KGTPVK) that could potentially interact with the negatively charged C-terminal tubulin tails. Interestingly, embedded in these four C-terminal repeats are seven consensus CDK1 phosphorylation sites; modification of these sites could reverse these charge–charge interactions and explain why this protein is not seen on microtubules in mitotic cells. A recent paper showed that altering the levels of Spindly in migrating border cells in the oocyte alters their migration speed (Clemente et al., 2017), suggesting that a role in migration is shared between *Drosophila* and human Spindly.

Human Spindly is primarily a nuclear protein in interphase cells, and before this report had not been shown to have any interphase role. Human Spindly lacks the charged regions seen in the *Drosophila* protein and is much less regularly observed on microtubules. Therefore, the particles that we observed moving on plus-ends or near the cortex were probably not directly bound to microtubules, but could be associated either with vesicles, plus-tip proteins, or other microtubule binding complexes. A recent publication has reported that CENP-F can also be seen associating with microtubule plus-ends, and so it may be that a subset of kinetochore proteins associate with microtubule cargoes to help them attach to plus-ends (Kanfer et al., 2017). Additionally, Spindly can now be considered like Zw10 and Mad1 as a kinetochore protein that has additional roles outside of mitosis (Wan et al., 2014; Schmitt, 2010).

Given that our data shows that the wild-type Spindly protein can rescue migration but the S256A dynactin-binding deficient point mutant cannot, we favour a model in which one or a few particular dynein/dynactin functions in migrating cells require Spindly. Observing Spindly enriching in the proximity of focal adhesions at the leading edge may also indicate a role for Spindly in cell adhesion, a process that has already been shown to be influenced by dynein/dynactin activity (Rosse et al., 2012). Future experiments to measure cell adhesion and/or contractility in the absence of Spindly will be needed to test whether Spindly has a role in regulating this process. However, this report represents a significant advance in our understanding of Spindly's role in interphase cells.

MATERIALS AND METHODS
Cell culture, transfection and RNA interference
U2OS cells and human foreskin fibroblast (FB) cells (a gift from Prof. A. Huebner, Technische Universitat Dresden, Dresden, Germany) were maintained in Opti-MEM (Thermo Fisher Scientific) supplemented with 10% heat-inactivated fetal bovine serum (HI-FBS) (Thermo Fisher Scientific), 1% Penicillin, Streptomycin and Glutamine (Thermo Fisher Scientific) for no more than 30 passages. Cell lines were grown at 37°C with 5% CO_2 in a humidified incubator.

To generate stable cell lines expressing wild-type or mutant (S256A) GFP-Spindly, U2OS cells with an integrated FRT site and a Tet repressor (a gift from Prof. A. Lamond, University of Dundee), were co-transfected with the pOG44 vector (a gift from Prof. J. R. Swedlow, University of Dundee) together with the pCDNA5/FRT/TO LAP-Spindly constructs (Gassmann et al., 2010) in a ratio of 9:1 pOG44:pgLAP vector. Stable integrating cell lines were subsequently drug selected in media containing 150 µg/ml of Hygromycin (Millipore) and 15 µg/ml of Blasticidin, and clonally isolated.

Expression of the GFP construct was induced by administration of doxycycline (0.1-1 µg/ml; Millipore).

DNA transfection procedure was carried out using the FuGene HD reagent (Promega, Madison, USA) according to manufacturer's instructions. Cells were transfected 24 h after being seeded with a FuGene/DNA ratio of 3:1 incubated in 200 µl of serum-free media for 30 min at room temperature.

The mix was dropped onto cells growing in OptiMEM supplemented with 10% FBS and plates were incubated at 37°C for at least 24 h before experiments were conducted. All the DNA plasmids used in this study were purified using the QIAprep Spin Miniprep Kit (Qiagen), following the manufacturer's instructions.

Small interfering RNA oligonucleotides were synthesized by SIGMA and transfected into cells using Lipofectamine RNAiMax (Thermo Fisher Scientific) according to the manufacturer's instructions. The oligonucleotide sequences used for siRNA knockdown are as follows: a GC-matched non-targeting control (MISSION Negative Control, SIGMA; Millipore) diluted to a final concentration of 20 nM; Spindly Endo1 (GA-AAGGGUCUCAAACAGAA) and Spindly-UTR-66 (CUUGAUCUGAC-AUAUAUCA) (neither of which target the expressed Spindly constructs) combined together to a final concentration of 20 nM. Cells were seeded and directly treated. Treatment was left on for 96 h and then cells were either fixed, harvested or seeded again for the subsequent analysis.

Western blotting and cell fractionation experiment
To perform the immunoblot analysis, cells were lysed using the following lysis buffer: 50 mM Tris/HCl pH 7.5, 150 mM NaCl, 100 mM N-Ethylmaleimide (NEM), 0.3% CHAPS, 1 mM EGTA, 1 mM EDTA, 10 mM Na-β-glycerophosphate, 1 mM Na-orthovanadate, 50 mM Na-Fluoride, 10 mM Na-pyrophosphate, 270 mM sucrose, 0.1 mM PMSF, 1 mM Benzamidine, 0.1% β-mercaptoethanol, 1 protease inhibitor cocktail tablet (Roche Diagnostics, Basel, Switzerland) for 10 ml of buffer. Cells were then transferred into Eppendorf tubes and put under constant agitation for 10 min at 4°C. Samples were subsequently spun down for 15 min at 13,000 rpm at 4°C. Supernatants were collected and stored at −80°C. Protein concentration was measured using Bradford dye (BioRad), according to the manufacturer's instructions. Samples were prepared in 2× loading buffer (Novex LDS sample buffer; Thermo Fisher Scientific) and boiled at 95°C for 5 min. Soluble fractions were resolved on Tris-glycine SDS-PAGE gels (4–12% gradient gel; Thermo Fisher Scientific) and transferred to a nitrocellulose membrane. Spindly, tubulin, geminin, GAPDH and PCNA were detected using specific antibodies: rabbit anti-Spindly (Griffis et al., 2007), mouse anti-PCNA, mouse anti-GAPDH, and rabbit anti-geminin from Santa Cruz Biotechnology, rat anti-tubulin from Thermo Fisher Scientific, sheep anti-GFP from Novus Biological (Abingdon, UK). The proteins were then visualised using ECL solution (Thermo Fisher Scientific).

To perform cell fractionation U2OS cells were grown to confluence in a 150 mm petri dish, washed with chilled PBS 1× and lysed in 200 µl of Buffer A (10 mM HEPES, pH7.9, 10 mM KCl, 1.5 mM $MgCl_2$, 1 mM DTT, 0.5 µg/µl Leupeptin, 0.5 µg/µl Aprotinin, 0.5 µg/µl Pepstatin, 0.1 mM PMSF, 0.34 M sucrose, 10% Glycerol, 0.1% Triton X-100, 1 µl DTT, 1 µl LPC), swirled and placed on ice for 20 min. Cells were then scraped, transferred to Eppendorf tubes and spun down at 1400 RCF for 10 min at 4°C. Supernatant was removed and collected into a new Eppendorf tube as the 'cytoplasmic' fraction. To the remaining pellet we added 50 µl of Buffer A combined with 0.2 µl benzonase nuclease (Millipore) and 10 µl 0.1 M $CaCl_2$ and incubated at 37°C for 1 min. The sample was then placed back on ice and supplemented with 0.2 µl of 0.5 M EGTA and incubated for 5 min. We then spun down the sample at 1400 RCF for 5 min at 4°C. The supernatant was removed and collected into a new Eppendorf tube as the 'nuclear' fraction.

Immunofluorescence microscopy
Cells were seeded onto sterilised glass coverslips (Menzel-Glaser, Braunschweig, Germany). When confluent, cells were fixed in 4% PFA in 1× PHEM (60 mM PIPES, 25 mM HEPES, 10 mM EGTA, 2 mM $MgCl_2$, pH 6.9) for 10 min at room temperature, washed in PHEM-wash (1× PHEM+0.1% Triton X-100), permeabilized in PHEM-T (1× PHEM+0.5% Triton X-100) for 5 min and fixed again in 4% PFA for 10 min. Blocking of non-specific antigen recognition was performed in Abdil (1× TBS-0.1% Tween, 2% BSA) for 1 h. At this point coverslips were incubated with primary antibodies for 1 h at room temperature or overnight at 4°C (antibodies were diluted in Abdil). The following antibodies and probes were used: phalloidin-Atto 488 (Millipore), mouse anti-p50 (Clone 25;

BD Biosciences), rabbit anti-pMyosin light chain (mAb 3675; Cell Signaling Technology), rabbit anti-pericentrin (ABT59; Millipore) and rabbit anti-Spindly (Griffis et al., 2007). Following incubation for 1 h with cross-subtracted secondary antibodies [either AlexaFluor-labelled (Thermo Fisher Scientific) or Cy3 or Cy5-labelled (Jackson ImmunoResearch)] diluted in Abdil with DAPI (Millipore). Antibody incubations were followed by three washes with PHEM-wash. Coverslips were mounted in Dako fluorescence mounting medium (Agilent Technologies, Santa Clara, USA). Images were collected using a fluorescence microscope (DeltaVision Elite; GE Healthcare). Images were then processed using OMERO software.

Cell migration assay and scratch assay

U2OS cells were treated for 96 h with either negative-control or Spindly-specific oligonucleotides, seeded into a silicone culture-insert (ibidi, Matinsried, Germany) set into a 35 mm μ-Dish (ibidi) and left to grow for at least 24 h. Once cells were confluent, the insert was removed and cells were washed once with fresh media and then the media was replaced with a CO_2 independent media (Leibovitz's L-15, supplemented with 10% FBS and 1× Penicillin/Streptomycin/Glutamine; Thermo Fisher Scientific). A sample of the cell population was collected for western blotting to confirm the silencing of Spindly. For blocking the cell cycle, cells were treated with hydroxyurea (HU) (1 mM; Millipore) for 24 h before being imaged, and a sample of the cell population was collected for western blotting to confirm silencing of Spindly and S-phase synchronisation. For the rescue experiments U2OS cells stably and inducibly expressing wild-type or S256A GFP-Spindly were treated with siRNAs that targeted either the endogenous Spindly or nothing. Subsequently, doxycycline (100 ng/ml) was administrated overnight to induce expression of the GFP construct, and a small portion of the cell population was harvested for western blotting to observe depletion of the endogenous Spindly and the expression of the GFP-tagged proteins.

Imaging was performed on a Nikon Ti microscope (Nikon, Tokyo, Japan) fitted with an environmental control chamber (Okolab, Pozzuoli, Italy), 20×0.45NA objective, Nikon PerfectFocus System, and a Photometrics Cascade II camera (Photometrics, Tucson, USA) and NIS Elements software. Images were then processed using Fiji software. Measurements were conducted by drawing a line between the edges and measuring the distance at the indicated time points. Kymograph analyses were conducted using Volocity software (Perkin Elmer; Waltham, USA) to measure the velocity of movement over the time. Student's t-test was used to determine the statistical significance of migration speeds and wound closure dimensions.

Human fibroblast cells were seeded onto glass coverslip and left grow until confluent. Then a scratch was mechanically generated by using a 200 μl tip and slides were fixed at different times to check for protein recruitment at the leading edge. Staining was performed as above.

TIRF imaging

Cells were grown and transfected in ibidi μ-Dishes; 2 h prior to imaging, the media was removed and replaced with a CO_2 independent Leibovitz's L-15 media without Phenol Red to lower autofluorescence. Imaging was performed on a Nikon Ti-E microscope with an environmental control chamber (Okolab), a PAU/TIRF slider, 63× and 100×1.49 N.A. objectives, PerfectFocus system, a custom-built four-color (405 nm, 488 nm, 561 nm, 647 nm) diode laser (Coherent Inc., Santa Clara, USA) system that has a Gooch and Housego (Ilminster, UK) AOTF shutter (Solamere Technology, Salt Lake City, USA), an emission filter wheel (Nikon) with appropriate filters for eliminating crosstalk between channels (Chroma Technology Corp, Bellow Falls, USA) and a Photometrics Evolve Delta camera (Tucson, USA). Images were all captured with μ-Manager (Open Imaging Inc., San Francisco, USA). In order to better visualize the moving particles of Spindly among the basal fluorescence, we utilized a method that was developed for tracking particles within Drosophila oocytes (Parton et al., 2011). Briefly, images were de-noised with a 3D Gaussian blur filter with a radius of 1 pixel. A temporal median filter was then used to extract only moving 'foreground' features using a sliding time window (half-width=4), and 'foreground' set to 4 standard deviations over the median value. The outputs of the temporal filter were then trailed using a sliding window of

time-points (half-width=2) and averaged to make moving particle trails obvious in all still frames. The temporal median filter plugin and trails plugin were created by Graeme Ball (https://github.com/graemeball/IJ_Temporal).

References
Akhshi, T. K., Wernike, D. and Piekny, A. (2014). Microtubules and actin crosstalk in cell migration and division. *Cytoskeleton* **71**, 1-23.
Aratyn-Schaus, Y., Oakes, P. W. and Gardel, M. L. (2011). Dynamic and structural signatures of lamellar actomyosin force generation. *Mol. Biol. Cell* **22**, 1330-1339.
Bachmann, A. and Straube, A. (2015). Kinesins in cell migration. *Biochem. Soc. Trans.* **43**, 79-83.
Barisic, M., Sohm, B., Mikolcevic, P., Wandke, C., Rauch, V., Ringer, T., Hess, M., Bonn, G. and Geley, S. (2010). Spindly/CCDC99 is required for efficient chromosome congression and mitotic checkpoint regulation. *Mol. Biol. Cell* **21**, 1968-1981.
Bernier, G., Pool, M., Kilcup, M., Alfoldi, J., de Repentigny, Y. and Kothary, R. (2000). Acf7 (MACF) is an actin and microtubule linker protein whose expression predominates in neural, muscle, and lung development. *Dev. Dyn.* **219**, 216-225.
Brandt, D. T. and Grosse, R. (2007). Get to grips: steering local actin dynamics with IQGAPs. *EMBO Rep.* **8**, 1019-1023.
Campellone, K. G. and Welch, M. D. (2010). A nucleator arms race: cellular control of actin assembly. *Nat. Rev. Mol. Cell Biol.* **11**, 237-251.
Chan, Y. W., Fava, L. L., Uldschmid, A., Schmitz, M. H. A., Gerlich, D. W., Nigg, E. A. and Santamaria, A. (2009). Mitotic control of kinetochore-associated dynein and spindle orientation by human Spindly. *J. Cell Biol.* **185**, 859-874.
Cheerambathur, D. K., Gassmann, R., Cook, B., Oegema, K. and Desai, A. (2013). Crosstalk between microtubule attachment complexes ensures accurate chromosome segregation. *Science* **342**, 1239-1242.
Clemente, G. D., Hannaford, M. R., Beati, H., Kapp, K., Januschke, J., Griffis, E. R. and Muller, H. J. (2018). Requirement of the Dynein-Adaptor Spindly for Mitotic and Post-Mitotic Functions in Drosophila. *J. Dev. Biol.* **6**.
Cianfrocco, M. A., Desantis, M. E., Leschziner, A. E. and Reck-Peterson, S. L. (2015). Mechanism and regulation of cytoplasmic dynein. *Annu. Rev. Cell Dev. Biol.* **31**, 83-108.
Duellberg, C., Trokter, M., Jha, R., Sen, I., Steinmetz, M. O. and Surrey, T. (2014). Reconstitution of a hierarchical +TIP interaction network controlling microtubule end tracking of dynein. *Nat. Cell Biol.* **16**, 804-811.
Faulkner, N. E., Dujardin, D. L., Tai, C.-Y., Vaughan, K. T., O'connell, C. B., Wang, Y. and Vallee, R. B. (2000). A role for the lissencephaly gene LIS1 in mitosis and cytoplasmic dynein function. *Nat. Cell Biol.* **2**, 784-791.
Firat-Karalar, E. N. and Welch, M. D. (2011). New mechanisms and functions of actin nucleation. *Curr. Opin. Cell Biol.* **23**, 4-13.
Folker, E. S., Baker, B. M. and Goodson, H. V. (2005). Interactions between CLIP-170, tubulin, and microtubules: implications for the mechanism of Clip-170 plus-end tracking behavior. *Mol. Biol. Cell* **16**, 5373-5384.
Gassmann, R., Essex, A., Hu, J.-S., Maddox, P. S., Motegi, F., Sugimoto, A., O'rourke, S. M., Bowerman, B., Mcleod, I., Yates, J. R.III et al. (2008). A new

mechanism controlling kinetochore-microtubule interactions revealed by comparison of two dynein-targeting components: SPDL-1 and the Rod/Zwilch/Zw10 complex. *Genes Dev.* **22**, 2385-2399.

Gassmann, R., Holland, A. J., Varma, D., Wan, X., Civril, F., Cleveland, D. W., Oegema, K., Salmon, E. D. and Desai, A. (2010). Removal of Spindly from microtubule-attached kinetochores controls spindle checkpoint silencing in human cells. *Genes Dev.* **24**, 957-971.

Gomes, E. R., Jani, S. and Gundersen, G. G. (2005). Nuclear movement regulated by Cdc42, Mrck, myosin, and actin flow establishes MTOC polarization in migrating cells. *Cell* **121**, 451-463.

Gotlieb, A. I., May, L. M., Subrahmanyan, L. and Kalnins, V. I. (1981). Distribution of microtubule organizing centers in migrating sheets of endothelial cells. *J. Cell Biol.* **91**, 589-594.

Gotlieb, A. I., Subrahmanyan, L. and Kalnins, V. I. (1983). Microtubule-organizing centers and cell migration: effect of inhibition of migration and microtubule disruption in endothelial cells. *J. Cell Biol.* **96**, 1266-1272.

Griffis, E. R., Stuurman, N. and Vale, R. D. (2007). Spindly, a novel protein essential for silencing the spindle assembly checkpoint, recruits dynein to the kinetochore. *J. Cell Biol.* **177**, 1005-1015.

Holland, A. J., Reis, R. M., Niessen, S., Pereira, C., Andres, D. A., Spielmann, H. P., Cleveland, D. W., Desai, A. and Gassmann, R. (2015). Preventing farnesylation of the dynein adaptor Spindly contributes to the mitotic defects caused by farnesyltransferase inhibitors. *Mol. Biol. Cell* **26**, 1845-1856.

Huber, F., Boire, A., López, M. P. and Koenderink, G. H. (2015). Cytoskeletal crosstalk: when three different personalities team up. *Curr. Opin. Cell Biol.* **32**, 39-47.

Kanfer, G., Peterka, M., Arzhanik, V. K., Drobyshev, A. L., Ataullakhanov, F. I., Volkov, V. A. and Kornmann, B. (2017). CENP-F couples cargo to growing and shortening microtubule ends. *Mol. Biol. Cell* **28**, 2400-2409.

Karakesisoglou, I., Yang, Y. and Fuchs, E. (2000). An epidermal plakin that integrates actin and microtubule networks at cellular junctions. *J. Cell Biol.* **149**, 195-208.

Kaverina, I. and Straube, A. (2011). Regulation of cell migration by dynamic microtubules. *Semin. Cell Dev. Biol.* **22**, 968-974.

Krause, M. and Gautreau, A. (2014). Steering cell migration: lamellipodium dynamics and the regulation of directional persistence. *Nat. Rev. Mol. Cell Biol.* **15**, 577-590.

Krendel, M., Zenke, F. T. and Bokoch, G. M. (2002). Nucleotide exchange factor GEF-H1 mediates cross-talk between microtubules and the actin cytoskeleton. *Nat. Cell Biol.* **4**, 294-301.

Magdalena, J., Millard, T. H. and Machesky, L. M. (2003). Microtubule involvement in NIH 3T3 Golgi and MTOC polarity establishment. *J. Cell Sci.* **116**, 743-756.

Mcgarry, T. J. and Kirschner, M. W. (1998). Geminin, an inhibitor of DNA replication, is degraded during mitosis. *Cell* **93**, 1043-1053.

Mckenney, R. J., Huynh, W., Tanenbaum, M. E., Bhabha, G. and Vale, R. D. (2014). Activation of cytoplasmic dynein motility by dynactin-cargo adapter complexes. *Science* **345**, 337-341.

Mingle, L. A., Okuhama, N. N., Shi, J., Singer, R. H., Condeelis, J. and Liu, G. (2005). Localization of all seven messenger RNAs for the actin-polymerization nucleator Arp2/3 complex in the protrusions of fibroblasts. *J. Cell Sci.* **118**, 2425-2433.

Montenegro-Venegas, C., Tortosa, E., Rosso, S., Peretti, D., Bollati, F., Bisbal, M., Jausoro, I., Avila, J., Caceres, A. and Gonzalez-Billault, C. (2010). MAP1B regulates axonal development by modulating Rho-GTPase Rac1 activity. *Mol. Biol. Cell* **21**, 3518-3528.

Moudgil, D. K., Westcott, N., Famulski, J. K., Patel, K., Macdonald, D., Hang, H. and Chan, G. K. T. (2015). A novel role of farnesylation in targeting a mitotic checkpoint protein, human Spindly, to kinetochores. *J. Cell Biol.* **208**, 881-896.

Nagano, M., Hoshino, D., Koshikawa, N., Akizawa, T. and Seiki, M. (2012). Turnover of focal adhesions and cancer cell migration. *Int. J. Cell Biol.* **2012**, 310616.

Palazzo, A. F., Cook, T. A., Alberts, A. S. and Gundersen, G. G. (2001a). mDia mediates Rho-regulated formation and orientation of stable microtubules. *Nat. Cell Biol.* **3**, 723-729.

Palazzo, A. F., Joseph, H. L., Chen, Y.-J., Dujardin, D. L., Alberts, A. S., Pfister, K. K., Vallee, R. B. and Gundersen, G. G. (2001b). Cdc42, dynein, and dynactin regulate MTOC reorientation independent of Rho-regulated microtubule stabilization. *Curr. Biol.* **11**, 1536-1541.

Parsons, J. T., Horwitz, A. R. and Schwartz, M. A. (2010). Cell adhesion: integrating cytoskeletal dynamics and cellular tension. *Nat. Rev. Mol. Cell Biol.* **11**, 633-643.

Parton, R. M., Hamilton, R. S., Ball, G., Yang, L., Cullen, C. F., Lu, W., Ohkura, H. and Davis, I. (2011). A PAR-1-dependent orientation gradient of dynamic microtubules directs posterior cargo transport in the Drosophila oocyte. *J. Cell Biol.* **194**, 121-135.

Reiner, O., Carrozzo, R., Shen, Y., Wehnert, M., Faustinella, F., Dobyns, W. B., Caskey, C. T. and Ledbetter, D. H. (1993). Isolation of a Miller-Dicker lissencephaly gene containing G protein beta-subunit-like repeats. *Nature* **364**, 717-721.

Ridley, A. J. (2011). Life at the leading edge. *Cell* **145**, 1012-1022.

Rogers, S. L., Wiedemann, U., Häcker, U., Turck, C. and Vale, R. D. (2004). Drosophila RhoGEF2 associates with microtubule plus ends in an EB1-dependent manner. *Curr. Biol.* **14**, 1827-1833.

Rooney, C., White, G., Nazgiewicz, A., Woodcock, S. A., Anderson, K. I., Ballestrem, C. and Malliri, A. (2010). The Rac activator STEF (Tiam2) regulates cell migration by microtubule-mediated focal adhesion disassembly. *EMBO Rep.* **11**, 292-298.

Rosse, C., Boeckeler, K., Linch, M., Radtke, S., Frith, D., Barnouin, K., Morsi, A. S., Hafezparast, M., Howell, M. and Parker, P. J. (2012). Binding of dynein intermediate chain 2 to paxillin controls focal adhesion dynamics and migration. *J. Cell Sci.* **125**, 3733-3738.

Schlager, M. A., Hoang, H. T., Urnavicius, L., Bullock, S. L. and Carter, A. P. (2014). In vitro reconstitution of a highly processive recombinant human dynein complex. *EMBO J.* **33**, 1855-1868.

Schmitt, H. D. (2010). Dsl1p/Zw10: common mechanisms behind tethering vesicles and microtubules. *Trends Cell Biol.* **20**, 257-268.

Schmoranzer, J., Kreitzer, G. and Simon, S. M. (2003). Migrating fibroblasts perform polarized, microtubule-dependent exocytosis towards the leading edge. *J. Cell Sci.* **116**, 4513-4519.

Schmoranzer, J., Fawcett, J. P., Segura, M., Tan, S., Vallee, R. B., Pawson, T. and Gundersen, G. G. (2009). Par3 and dynein associate to regulate local microtubule dynamics and centrosome orientation during migration. *Curr. Biol.* **19**, 1065-1074.

Schroeder, C. M. and Vale, R. D. (2016). Assembly and activation of dynein-dynactin by the cargo adaptor protein Hook3. *J. Cell Biol.* **214**, 309-318.

Smith, D. S., Niethammer, M., Ayala, R., Zhou, Y., Gambello, M. J., Wynshaw-Boris, A. and Tsai, L.-H. (2000). Regulation of cytoplasmic dynein behaviour and microtubule organization by mammalian Lis1. *Nat. Cell Biol.* **2**, 767-775.

Stehbens, S. and Wittmann, T. (2012). Targeting and transport: how microtubules control focal adhesion dynamics. *J. Cell Biol.* **198**, 481-489.

Urnavicius, L., Zhang, K., Diamant, A. G., Motz, C., Schlager, M. A., Yu, M., Patel, N. A., Robinson, C. V. and Carter, A. P. (2015). The structure of the dynactin complex and its interaction with dynein. *Science* **347**, 1441-1446.

Valetti, C., Wetzel, D. M., Schrader, M., Hasbani, M. J., Gill, S. R., Kreis, T. E. and Schroer, T. A. (1999). Role of dynactin in endocytic traffic: effects of dynamitin overexpression and colocalization with CLIP-170. *Mol. Biol. Cell* **10**, 4107-4120.

Vasiliev, J. M., Gelfand, I. M., Domnina, L. V., Ivanova, O. Y., Komm, S. G. and Olshevskaja, L. V. (1970). Effect of colcemid on the locomotory behaviour of fibroblasts. *J. Embryol. Exp. Morphol.* **24**, 625-640.

Vaughan, K. T., Tynan, S. H., Faulkner, N. E., Echeverri, C. J. and Vallee, R. B. (1999). Colocalization of cytoplasmic dynein with dynactin and CLIP-170 at microtubule distal ends. *J. Cell Sci.* **112**, 1437-1447.

Vaughan, P. S., Miura, P., Henderson, M., Byrne, B. and Vaughan, K. T. (2002). A role for regulated binding of p150(Glued) to microtubule plus ends in organelle transport. *J. Cell Biol.* **158**, 305-319.

Wan, J., Zhu, F., Zasadil, L. M., Yu, J., Wang, L., Johnson, A., Berthier, E., Beebe, D. J., Audhya, A. and Weaver, B. A. (2014). A Golgi-localized pool of the mitotic checkpoint component Mad1 controls integrin secretion and cell migration. *Curr. Biol.* **24**, 2687-2692.

Waterman-Storer, C. M., Worthylake, R. A., Liu, B. P., Burridge, K. and Salmon, E. D. (1999). Microtubule growth activates Rac1 to promote lamellipodial protrusion in fibroblasts. *Nat. Cell Biol.* **1**, 45-50.

Yadav, S., Puri, S. and Linstedt, A. D. (2009). A primary role for Golgi positioning in directed secretion, cell polarity, and wound healing. *Mol. Biol. Cell* **20**, 1728-1736.

Yamamoto, T. G., Watanabe, S., Essex, A. and Kitagawa, R. (2008). SPDL-1 functions as a kinetochore receptor for MDF-1 in Caenorhabditis elegans. *J. Cell Biol.* **183**, 187-194.